

# Tilt Integral Derivative Controller Optimized by Battle Royale Optimization for Wind Generator Connected to Grid

Mohamed Samir<sup>1</sup>, Gagan Singh<sup>2</sup>, Nafees Ahamad<sup>3</sup>

<sup>1,2,3</sup>Department of Electrical and Electronics & Communication Engineering, DIT University, India

---

## Article Info

### Article history:

Received Jan 13, 2022

Revised Apr 26, 2022

Accepted May 19, 2022

### Keyword:

Doubly Fed Induction  
Generator Wind Farm,  
Antlion,  
Battle Royale,  
TID Controller,

---

## ABSTRACT

Globally the countries are focusing on reducing the carbon footprint leading to a greater effort for electrical energy generation by renewable energy sources, particularly wind. The wind turbines are invariably using doubly fed asynchronous generator. In this paper a controller has been designed for a doubly fed induction motor. The proposed Tilt Integral Derivate controller for was compared with commonly used PI, PID controllers. Several optimization algorithms were used for tuning of controllers and the best one was selected for each type of controller. The controller has been optimized using battlefield optimization. It had been compared with proportional integral controller, fractional order proportional integral derivative controller. Other controllers were optimized using meta heuristic algorithms. The controller enhanced the system response in terms of settling time, rise time and other parameters. The Tilt controller gave the overall superior performance in terms of parameters like rise time, settling time, settling minimum, peak, and peak time. The results were obtained using MATLAB. This paper discusses operation of doubly fed induction motor operation and optimization methods.

Copyright © 2022 Institute of Advanced Engineering and Science.  
All rights reserved.

---

## Corresponding Author:

Mohamed Samir,  
Department of Electrical and Electronics & Communication Engineering,  
DIT University,  
Mussoorie Diversion Road, Vill Makkawala, P.O. Bhagwantpur, Dehradun, Uttarakhand 248001, India.  
Email: [mohamed.samir@dituniversity.edu.in](mailto:mohamed.samir@dituniversity.edu.in)

---

## 1. INTRODUCTION

Low capital cost, small gestation period and no pollution are some of the advantages which has led to the development of wind power as one of the major sources of renewable energy. The new generation wind turbines are manufactured using advanced materials based on aerodynamic principles borrowed from aerospace industry.

Among all renewable sources of energy in the last 10 to 20 years, wind energy has developed rapidly [1] as the most worthwhile source for generating electrical energy [2]. Electrical energy generation from wind is now common in remote rural areas. The concept of doubly fed induction generator (DFIG) for electrical power generation is widely used when considering wind turbines operating at variable speed. [3]. The wind turbines being used can have two possible operating modes – constant speed or variable speed [4]. Previously FSWT (fixed speed wind turbine) were obvious choice, but they suffered from limitations such as lack of support for reactive power, low efficiency, mechanical stress on turbine and difficulty in extracting maximum power at variable speed [5]. The VSWT (variable speed wind turbine) offers better advantages like extracting maximum power at changing speed requiring a converter capable of operating at 25 percent to 30 percent of DFIG rated capacity [6].

A WECS consists of an electrical generator, blades, control system and a power electronic converter as shown in fig.1. The functional objective of WECS is conversion of kinetic energy into electrical energy which is injected into the load or grid. Different schemes have been proposed for wind turbine operation where

some schemes optimize its operation by estimation of wind speed. [7]. There are controllers which extract from a given wind system maximum power by using elaborate searching method [8][9] [10]. Several controllers have been used in the past for DFIG based WECS. The performance of a tilt integral derivative (TID) and fractional order proportional integral derivative (FOPID) controllers proposed in this paper have been evaluated for control of DFIG connected to the grid. In [3] different types of controllers were compared. Several topologies have been used for controlling speed of a wind generator. In most of the papers considered [3],[5], PI controllers based on classical control theory, PI controller along with the Fuzzy controller, the PI controller using heuristic algorithm, the PI controller using Genetic Algorithm (GA), PI controller using swarm optimization have been used. In [5] a PID controller using particle swarm optimization and bacterial foraging optimization were used. However although the controller showed improvements in terms of rise time, settling time and other parameters but the output obtained was not as desired. In [2] a fractional order PID controller behaviour has been analysed for a DFIG system. However it had been optimized using only FPID optimization tool of MATLAB. Only some of the parameters of the controller were compared with PID controller. In this paper we have tried to evaluate the performance of various controllers like PI, PID and FOPID but a new controller has been proposed. A number of optimization techniques have been used for the different controllers.

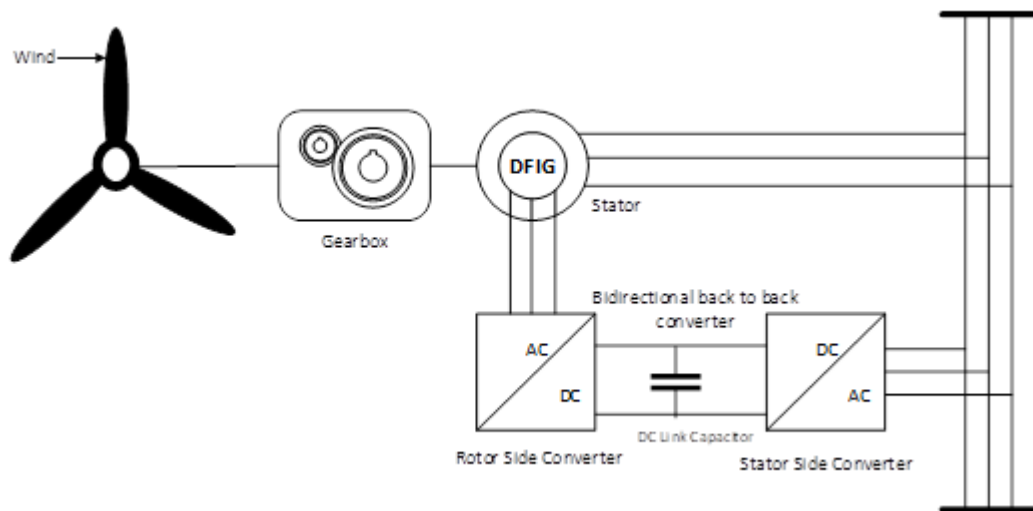


Figure 1. Wind Energy Conversion System

## 2. WIND FARM (WF) EQUIVALENT MODEL BASED ON TRANSFER FUNCTION

The changes in wind speed and faults in power system results in change in wind farm (WF) power output. In case of WF when a fault occurs then it results in steep decrease in terminal voltage as well as quick change in power output. The WF kinetics can be well described under both variable wind speed and fault in the system with the help of an equivalent model. The WF can be considered as a nonlinear equivalent impedance[11]. The WF equivalent model in terms of transfer function can be expressed as

$$P = P_o \left[ H_{pv} \left( \frac{V}{V_o} \right)^2 \right] \left[ H_{pw} \left( \frac{W}{W_o} \right)^3 \right] \quad (1)$$

$$Q = Q_o \left[ H_{qv} \left( \frac{V}{V_o} \right)^2 \right] \left[ H_{qw} \left( \frac{W}{W_o} \right)^3 \right] \quad (2)$$

where

- $P$  = WF output active power
- $Q$  = WF output reactive power
- $V$  = WF terminal voltage
- $V_o$  = WF terminal voltage initial value
- $W$  = wind speed (input)
- $W_o$  = wind speed (initial value)
- $H_{pv}$ ,  $H_{pw}$ ,  $H_{qv}$  and  $H_{qw}$  are transfer functions

The fig.2 and fig. 3 shows the configuration for the active and reactive power respectively

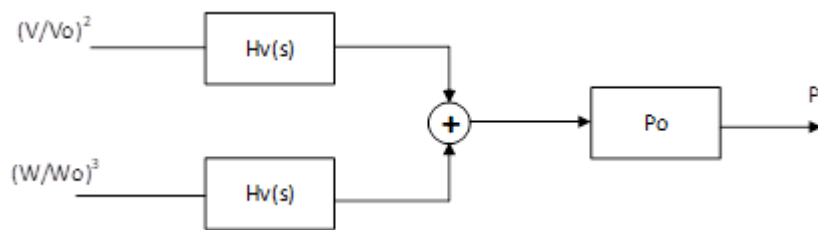


Figure 2. Configuration for the active power

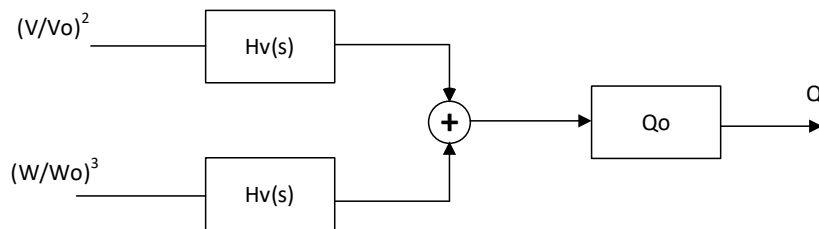


Figure 3. Configuration for the reactive power

The method based on transfer function considers WF as a black box. The accuracy of an equivalent model based on components is higher than transfer function-based model [11]. In a WF, no. of wind turbines (WTs) are used which must work in an orderly manner to aggregate them into an equivalent model [12]. In [11] a WF was built in MATLAB having 16 WTs which were connected to an infinite bus using two transmission lines. Particle swarm optimization (PSO) was used in estimating the parameters whose details are given in [13]. [14]. Reactive and active powers were recorded by a phasor measurement unit (PMU) as well as terminal voltage was measured for a WF using 20 WTs with DFIM in NW China.

### 2.1. Doubly Fed Induction Generator (DFIG) and its modelling

The power electronic converter plays crucial role in WECS particularly with variable speed control method. The configuration of WECS determines the capacity of power electronic converter. A rectifier-inverter pair is the most common configuration for the converters used in case of variable wind speed turbine system. [14] or matrix converter has the possibility of substituting rectifier-inverter pair structure. The adjoining rectifier inverter pair is a bidirectional power converter consisting of two conventional pulse width modulation (PWM) voltage source converter (VSC) [15] as shown in fig. 4

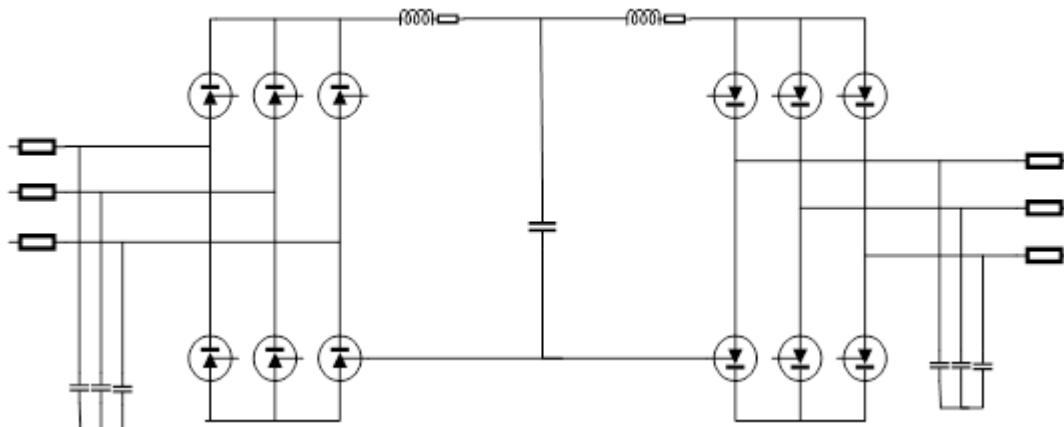


Figure 4. Back-to-Back rectifier inverter converter

Among two converters, one operates in rectification mode and the other in inverting mode being connected using a dc link utilizing a capacitor. The grid side converter (GSC) controls power flow keeping voltage constant. The converter at the generator side controls the generator allowing maximum power of the

wind to be directed towards d.c. bus [16]. A matrix converter is a single stage AC to AC converter having an array of nine bidirectional semiconductor switches connecting each input phase to each output phase and can be considered as alternate to the back-to-back converter.

The proper operation of switches connecting output and input terminals of the converter results in the frequency, voltage, displacement angle at the output as per the requirement. The Fig.5 [17] shows the components of a model of a wind turbine.

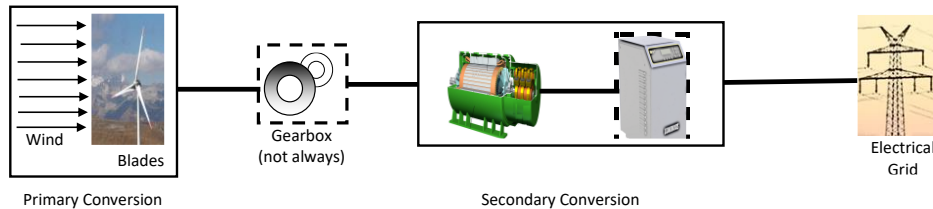


Figure 5. Components of a wind turbine model

The model of an induction machine in case of WECS mostly used is based on flux linkages [18]. Based on flux linkages in dq0 frame, the machine can be described by four differential equations as follows:

$$\frac{d\psi_{qs}}{dt} = C_1\psi_{qs} - \omega_e\psi_{ds} + C_2\psi_{qr} + \omega_b v_{qs} \quad (3)$$

$$\frac{d\psi_{ds}}{dt} = \omega_e\psi_{qs} + C_1\psi_{ds} + C_2\psi_{dr} + \omega_b v_{bs} \quad (4)$$

$$\frac{d\psi_{qs}}{dt} = C_3\psi_{qs} - C_4\psi_{qr} - (\omega_e - \omega_{re})\psi_{dr} \quad (5)$$

$$\frac{d\psi_{dr}}{dt} = C_3\psi_{ds} + (\omega_e - \omega_{re})\psi_{qr} + C_4\psi_{dr} \quad (6)$$

$$\frac{d\omega_{re}}{dt} = \left(\frac{p}{2J}\right)(T_e - T_L) \quad (7)$$

Where,

$\psi_{qs}$  &  $\psi_{ds}$  are flux linkages on stator side corresponding to both  $d$  and  $q$  axis

$\psi_{qr}$  &  $\psi_{dr}$  are flux linkages on rotor side corresponding to both  $d$  and  $q$  axis

$\omega_e$  is stator angular speed

$\omega_b$  is base angular speed

$p$  is number of poles

The control of converter on grid side is studied by developing a dynamic model based on space vector theory which uses a vector control technique which aligns space vector corresponding to grid voltage with a rotating reference frame (dq) which results in achieving power exchange for reactive power and control of DC bus voltage through the converter.

A stable model of wind power plant needs to be developed for study of a modern electric power system involving a wind power plant under steady state. Studies have been conducted mostly on this modelling [19] by many researchers. The most common used control approach for control at rotor side uses back-to-back bidirectional AC -AC power converter which assists in maintaining the rotor power frequency constant. [20] [21]. For achieving generator control, which is quick and decoupled, we can apply vector control technique. The rotating and complex three phase parameters like voltages, currents are converted to corresponding stationary DQ frame. The following equations are utilized for modelling of DFIG in synchronous d-q reference frame which rotates at a speed  $\omega_s$  [22]:

Stator Voltage Components:[23]

$$\begin{cases} V_{ds} = R_s I_{ds} + \frac{d}{dt}\psi_{ds} - \omega_s\psi_{qs} \\ V_{qs} = R_s I_{qs} + \frac{d}{dt}\psi_{qs} + \omega_s\psi_{ds} \end{cases} \quad (8)$$

Where  $V_{ds}$  = stator voltage (direct axis)

$V_{qs}$  = stator voltage (quadrature axis)

Rotor components: [23]

$$\begin{cases} V_{dr} = R_r I_{dr} + \frac{d}{dt} \psi_{dr} - (\omega_s - \omega_r) \psi_{qr} \\ V_{qr} = R_r I_{qr} + \frac{d}{dt} \psi_{qr} - (\omega_s - \omega_r) \psi_{dr} \end{cases} \quad (9)$$

Where  $V_{dr}$  = stator voltage (direct axis)  
 $V_{qr}$  = stator voltage (quadrature axis)

Stator flux components: [23]

$$\begin{cases} \psi_{ds} = L_s I_{ds} + L_m I_{dr} \\ \psi_{qs} = L_s I_{qs} + L_m I_{qr} \end{cases} \quad (10)$$

Where  $L_s$  = self-inductance on stator side  
 $L_m$  = mutual inductance

Rotor flux components: [23]

$$\begin{cases} \psi_{dr} = L_r I_{dr} + L_m I_{ds} \\ \psi_{qr} = L_r I_{qr} + L_m I_{qs} \end{cases} \quad (11)$$

Where  $L_r$  = self-inductance on rotor side

DFIG electromagnetic torque:[23]

$$T = \frac{3}{2} p \frac{L_m}{L_r} (\psi_{ds} I_{qr} - \psi_{qs} I_{dr}) \quad (12)$$

The active and reactive power at the stator end i.e.  $P_{stator}$  as well as reactive  $Q_{stator}$  are expressed as follows:

$$\begin{cases} P_{stator} = \frac{3}{2} (V_{ds} I_{ds} + V_{qs} I_{qs}) \\ Q_{stator} = \frac{3}{2} (V_{qs} I_{ds} - V_{ds} I_{qs}) \end{cases} \quad (13)$$

## 2.2. Simple model of DFIG

By positioning the stator flux along the d axis in d-q axis frame it is feasible to regulate for the converter at rotor end both powers i.e., active, and reactive. The DFIG model becomes simpler when we ignore stator resistance whereas the flux of stator is constant as it is directly being connected to grid. The above equations from 8 to 13 thus gets modified as follows:

$$\begin{cases} V_{ds} = 0 \\ V_{qs} = V_s = \omega_s \psi_s \end{cases} \quad (14)$$

$$\begin{cases} \psi_s = L_s I_{ds} + L_m I_{dr} \\ 0 = L_s I_{qs} + L_m I_{qr} \end{cases} \quad (15)$$

$$\begin{cases} I_{ds} = \frac{\psi_s}{L_s} - \frac{L_m}{L_r} I_{dr} \\ I_{qs} = -\frac{L_m}{L_s} I_{qr} \end{cases} \quad (16)$$

$$\begin{cases} P_s = \frac{3}{2} V_s I_{qs} \\ Q_s = \frac{3}{2} V_s I_{ds} \end{cases} \quad (17)$$

Where  $I_{ds}$  and  $I_{qs}$  are stator currents corresponding to both direct and quadrature axis

The expressions for powers - active & reactive in flux linkage terms are expressed by putting the values of stator currents from eq. (16) in eq. (17) as follows:

$$\begin{cases} P_s = -\frac{3 L_m}{2 L_s} V_s I_{qr} \\ Q_s = \frac{3}{2} V_s \left( \frac{\psi_s}{L_s} - \frac{L_m}{L_s} I_{dr} \right) \end{cases} \quad (18)$$

The electromagnetic torque accordingly is given by

$$T(\psi_s I_{qr}) = \frac{3}{2} p \frac{Lm}{Ls} \tag{19}$$

The rotor end voltages can be expressed as follows:

$$\begin{cases} V_{dr} = R_r I_{dr} - g\omega_s \left( L_r - \frac{Lm^2}{Ls} \right) I_{qr} \\ V_{qr} = R_r I_{dr} - g\omega_s \left( L_r - \frac{Lm^2}{Ls} \right) I_{dr} + g \frac{Lm}{Ls} V_s \end{cases} \tag{20}$$

**2.3. Simulink models of Controllers for DFIG (Transfer function based)**

The fig.6 to fig.9 shows the Simulink models of PI, PID, FOPID and TID controllers used in MATLAB/Simulink

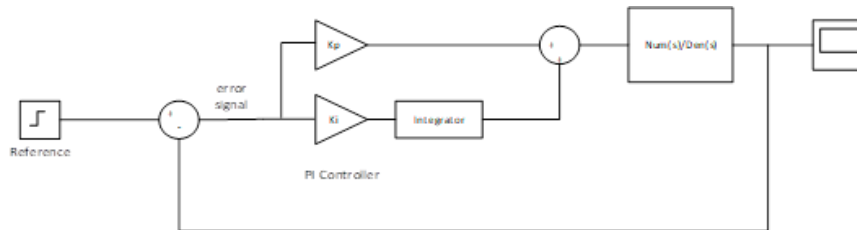


Figure 6. Simulink model of PI controller

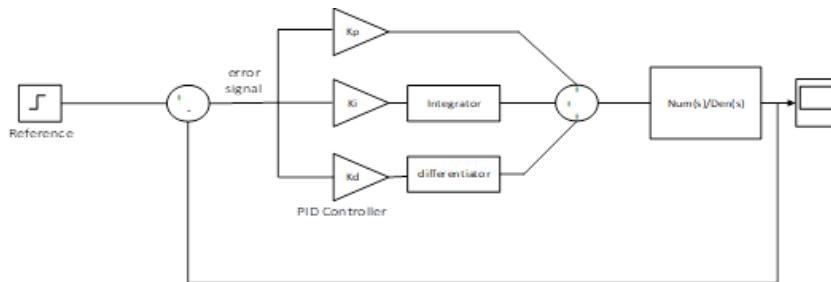


Figure 7. Simulink model of PID controller

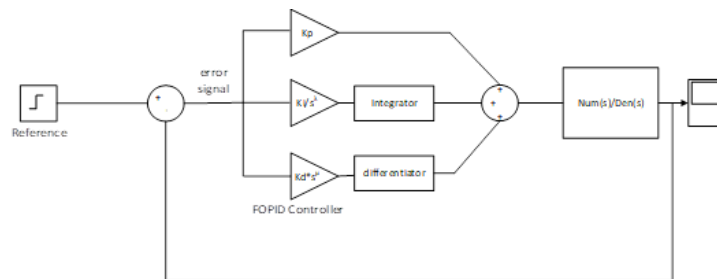


Figure 8. Simulink model of FOPID controller

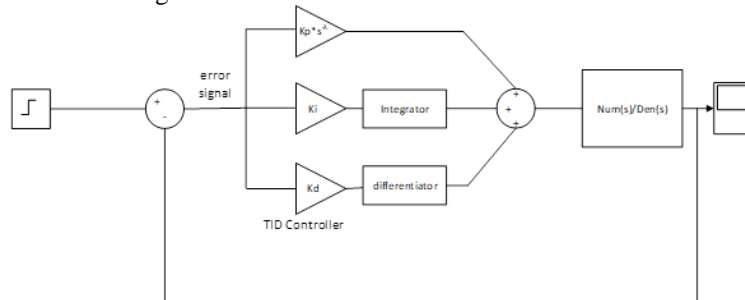


Figure 9. Simulink model of TID controller

## 2.4. Algorithms used for controller optimization

The method of determining the best solution in a set of workable solutions for a given problem is known as optimization [24]. In case of many engineering and industrial application, a crucial role is played by optimization algorithms[25]. Some of the algorithms like central force optimization (CFO) [26], gravitational search algorithm (GSA)[27], water evaporation optimization (WEO) [28] are inspired by physics. All the algorithms try to provide a balance between exploitation and exploration. Among the various algorithms several meta heuristic algorithms are used for solving complicated problems [29]. These algorithms inspired by nature in most cases such as Particle Swarm Optimization[30], Whale Optimization algorithm [31], Antlion Optimizer [32], Bat algorithm [33], Ant Colony optimization [34], Magnetic Charges System Search[35], Grey Wolf Optimizer [36], Harmony Search[37], League Championship algorithm [38], Dragonfly algorithm [39] etc. have been presented in literature. In the current paper we have used Battle Royale optimization (BRO), Antlion optimization (ALO) and Bat Optimization algorithm.

### 2.4.1. Antlion Optimization (ALO)

The ALO is based on the hunting method adopted by antlions for their favourite prey ants. Antlions during the full moon [40] or when they are hungrier, dig bigger traps. What should be the size of trap? This decision is taken based on its internal lunar clock.[40]. The antlion creates a pit for trapping the ants which is in the shape of a cone. The antlion while preparing the pit throws sand at its edge and makes it sharp to ensure that the prey is trapped easily and does not escape from it. There are five stages used to explain the hunting method of antlions[41]. The following points briefly explains the process of catching its prey by an antlion:

- The mobility of ants in search space is random.
- The arbitrary movement of ants influences the traps created by antlions.
- The size of pit is determined by the value of the fitness function and accordingly a pit is constructed.
- The best chance of trapping an ant is by the antlion having greater fitness value.
- The most fit antlion can trap the ant in each iteration.
- The drifting action of ants towards antlions is triggered by adjusting combination of random walks in diminishing order.
- An ant is considered being trapped by an antlion if the antlion has a less fitness value as compared to an ant.
- The antlion after every hunt changes its position.

### 2.4.2. Bat Optimization

In 2010 Yang introduced an algorithm based on echolocation behaviour of microbats [33]. A bat detects its prey by producing an extremely high sound which echoes back with same frequency. The process of detecting an object with the help of sound being reflected is called echolocation. The bats are capable enough of differentiating between its prey and an obstacle by observing the reflected frequency of sound. The bats can differentiate between targets as the fluttering of insect wings result in variation of Doppler effect [42]. The following rules are used in case of bat optimization algorithm:

- Echolocation is utilized to sense distance and help them in differentiating between prey and background barrier.
- Bats fly in a haphazard manner with velocity  $w_i$  at a stable frequency  $f_{min}$  at position  $y_i$  with loudness  $A_0$  and wavelength  $\lambda$  which varies when searching for prey. The pulse emission rate and frequency are automatically adjusted based on the closeness of its target.
- The loudness differs between a minimum fixed value and a large value.

### 2.4.3. Battle Royale Optimization (BRO)

The method of determining the best solution in a group of workable solutions for a given problem is known as optimization [24]. In case of many engineering and industrial applications a crucial role is played by optimization algorithms. Several optimization problems in the past few years utilized metaheuristic algorithms [25]inspired by Darwin's evolution theory. Some of the algorithms like central force optimization (CFO)[26] , gravitational search algorithm (GSA)[27], water evaporation optimization (WEO) [28] are inspired by physics. All the algorithms try to provide a balance between exploitation and exploration. In 2020, T.R. Farshi proposed an optimization algorithm based on a game strategy inspired by battle royal video games called battle royale optimization (BRO).

The BRO starts with a random population which is scattered in the space problem uniformly. Then each soldier/player uses a weapon to shoot the other nearest soldier. The soldier in better position causes damage to another soldier and all this can be expressed mathematically as

$$X_{dm,d} = X_{dm,d} + r(X_{b,d} - X_{dm,d})$$

where  $r$  = randomly generated number distributed uniformly in  $[0,1]$   
 $X_{m,d}$  = position of hurted soldier in dimension  $d$

The damage is set to zero in the next iteration if a hurt soldier is still capable of damaging his opponent. When the damage of soldier exceeds the threshold value, he/she dies and is regenerated randomly from the likely problem space to offer better exploration and convergence.

$$X_{d,m} = 0$$

The soldier who comes back after being killed is represented as

$$X_{dm,d} = r(u_d - I_d) + I_d$$

where  $u_d$  and  $I_d$  are the upper and lower limits of dimension  $d$ .

With each iteration the search space goes on shrinking towards the best solution. The number of iterations is related to a particular iteration as

$$\begin{aligned} \text{delta} &= \log 10 (\text{maxcircle}) \\ \text{delta} &= \text{delta} + \text{round} \left( \frac{\text{delta}}{2} \right) \end{aligned}$$

where *maxcircle* is maximum number of generations.

The upper and lower limits are updated as

$$I_d = X_{bes,d} - SD(X_d)$$

$$u_d = X_{bes,d} + SD(X_d)$$

where  $SD(X_d)$  is standard deviation of entire population in dimension  $d$

## 2.5. Fractional Order PID (FOPID) Controller

Being an old branch of mathematics, fractional calculus was previously studied in mathematics only. However, since last few years it has gained an acceptance in many engineering applications[43]. Several applications like DC motor speed control[44], robotics [45], aero fin control system [47] have used FOPID controllers. In terms of time and frequency domain a fractional order proportional integral derivative (FOPID) controller designated as  $PI^\lambda D^\mu$  controller is given by

$$G_c(t) = K_p e(t) + K_i D_t^{-\lambda} e(t) + K_d D_t^\mu e(t) \quad (21)$$

$$G_c(s) = K_p + K_i s^{-\lambda} + K_d s^\mu \quad (22)$$

where  $0 < \lambda < 2, 0 < \mu < 2$

The PID controller owing to its simplicity in design and effective performance has been used in many industrial applications successfully for decades[46]. The FOPID controller was introduced in 1997 [47] [48] [49] which can be considered as general form of conventional PID controller. Such a controller was tuned using Ziegler Nichols[50]. Additionally, many new tuning algorithms were proposed in[51] [52]. The complexity of this controller is more compared to conventional PID controller as the number of control parameters increase to five ( $K_p, K_i, K_d, \lambda, \mu$ ) instead of three as in PID controller but it helps in achieving design requirements like errors in steady state, phase margin and gain margin as per the requirements.

## 2.6. Tilt Integral Derivative (TID) Controller

Several controllers like proportional integral (PI), proportional integral derivative (PID) has been used in WECS. The tilt integral derivative (TID) controller provides a better response compared to a conventional



PID controller. In case of TID controller, the proportional component is replaced with a compensator having a transfer function  $s^{-1/n}$  where  $n$  is a real number other than zero. In comparison to conventional proportional compensator, the overall response is close to the optimal response determined by Bode when it is replaced with the tilt compensator [53]. In addition to many advantages of conventional PID controller which includes easier tuning, a TID controller also maintains the general structure of PID controller. The three parallel paths have gains which can be tuned such that the gain response and phase shift are not dependent on frequency. This makes TID controller easily implementable in plants with different bandwidth. Having a transfer function involving  $s$  or power of  $s$  ensures that TID controller is considerably universal [54].

The advantages of TID controller over conventional PID controllers are tuning is simple, effect of variation in plant parameters is small, rejection ratio for disturbance is better. The main objective of a TID controller is to provide a response close to optimal response [55].

### 3. RESULTS AND DISCUSSION

For PID and FOPID controllers the following initial parameters were used:

Parameters	PID Controller	FOPID Controller	TID Controller
$K_p$	10	15	20
$K_i$	10	18	15
$K_d$	1	5	10
$N$	-	-	0.4
$\lambda$	-	0.3	-
$\mu$	-	0.3	-

The following parameters were selected for the Optimization method:

Parameters	Antlion Optimization	Bat Optimization	Battle Royal Optimization
No. of search agents	45	10	10
No. of maximum iterations	50	100	200
Lower bound	1/1000	1/100	1/100
Upper bound	100	200	[1 500 500 1]

The ALO gives the best result as:

For PID controller

$K_p = 0.75634$ ,  $K_i = 9.6084$ ,  $K_d = 2.546$

For FOPID controller

$K_p = 0.75634$ ,  $K_i = 9.6084$ ,  $K_d = 2.546$ ,

$\lambda = 0.04$ ,  $\mu = 0.03$

The following results were obtained corresponding to open loop (without controller) step response

Rise Time (in sec.) = 159.6685

Settling Time (in sec.) = 264.142

Settling Minimum = 0.9603

Settling Maximum = 0.999

Overshoot = 0

Undershoot = 0

Peak = 0.999

Peak Time (in sec.) = 507.5658

The table 1 shows the comparison between the step response of open loop system for the given wind turbine and other controllers used with different optimization techniques

Table 1. Performance of PI, PID, FOPID and TID Controllers

Parameters	System Without Controller	PI Controller Optimized using Bat Optimization	PID Controller Optimized using ALO	FOPID Controller Optimized using ALO	TID Controller Optimized using BRO
Rise Time	50.9554	116.4686	45.678	0.7407	0.2484
Settling Time	81.8459	4.993	60.6753	6.75	4.0976
Settling Min	0.4673	1.2783	0.9592	0	0.6695
Settling Max	0.4775	0	1.007	2	1.6131
Overshoot	0	27.8289	0.6974	1.2	61.3143
Undershoot	0	0	0	0	0
Peak	0.4775	1.2783	1.007	27	1.6131
Peak Time	100	21.8378	12.9871	1	0.6

The fig. 10 to fig. show the performance behaviour of the various controllers discussed in the paper with respect to active power, reactive power, stator side voltages, stator side currents, rotor side voltages, rotor side currents and dc bus voltage.

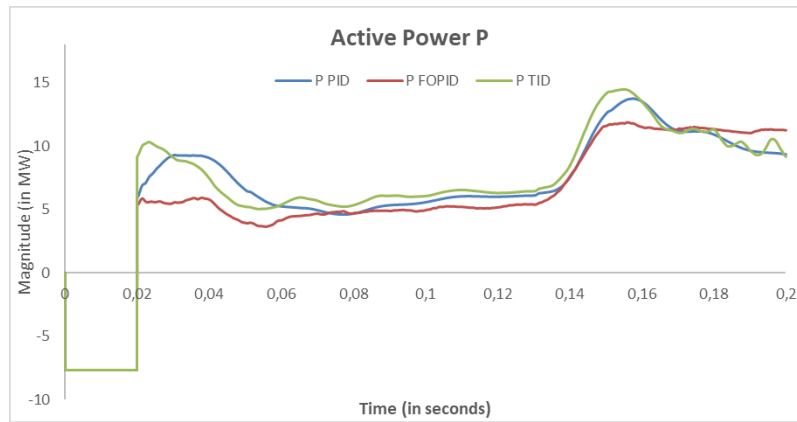


Figure 10. Active Power

As can be seen from the figure corresponding to active power it can be clearly seen that TID controller provides more active power as compared to PID and FOPID controllers. The average active power for DFIG using TID controller is 6.627 MW which is 5% more than FOPID (6.3 MW) and 18 % more than PID (5.6 MW). Thus, with respect to active power TID gave the best performance.

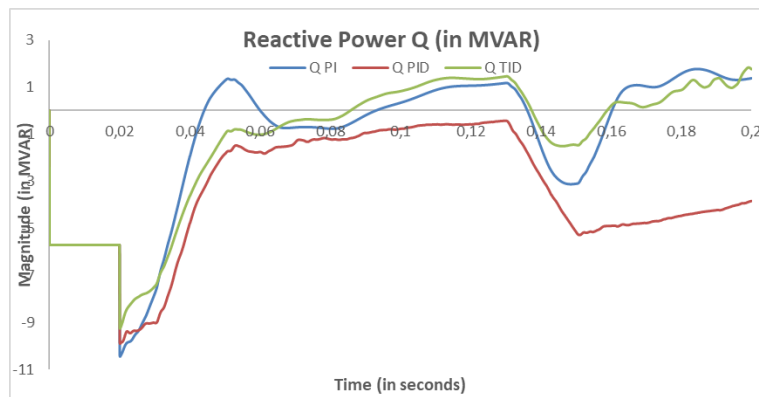


Figure 11. Reactive Power

It has been observed that in the case of DFIG model considered the reactive power required is negative since DFIG is being used. As can be seen from the concerned graphs that TID gave better performance than both PI and PID controllers.

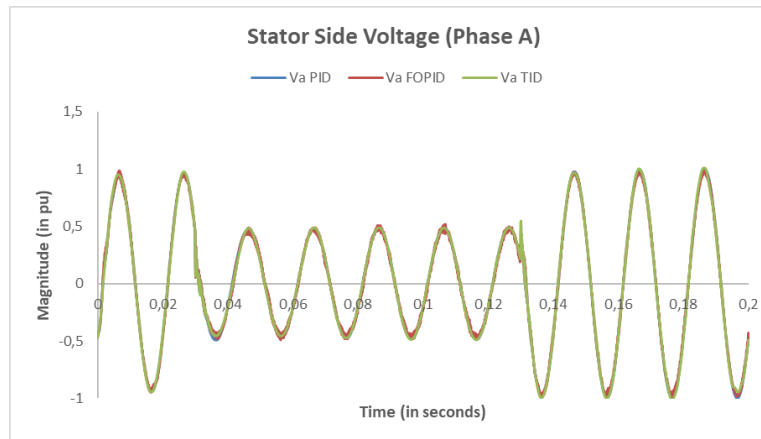


Figure 12. Stator Voltage for Phase A

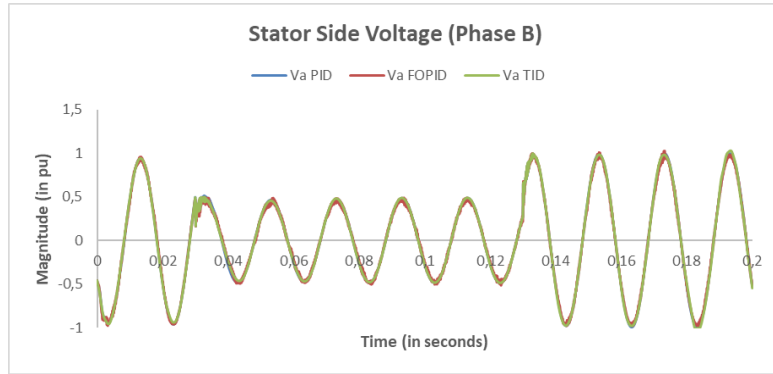


Figure 13. Stator Side Voltage for Phase B

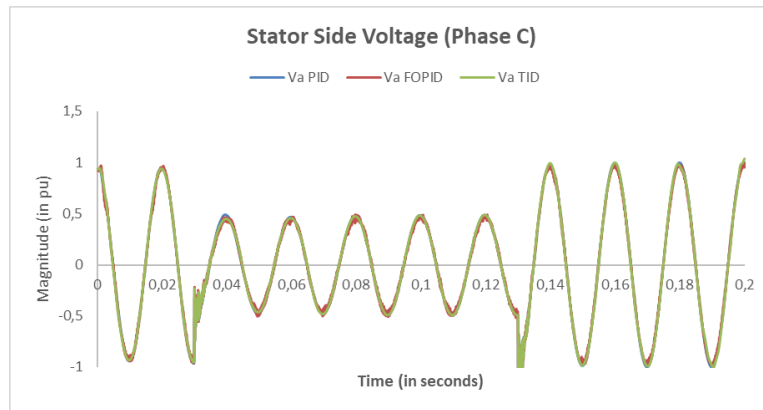


Figure 14. Stator Side Voltage for Phase C

In case of stator voltages for all the phases it can be seen from fig.12 to fig. 14 that the response is the same for all the different types of controllers. However, the voltages have less harmonics in case of TID controller

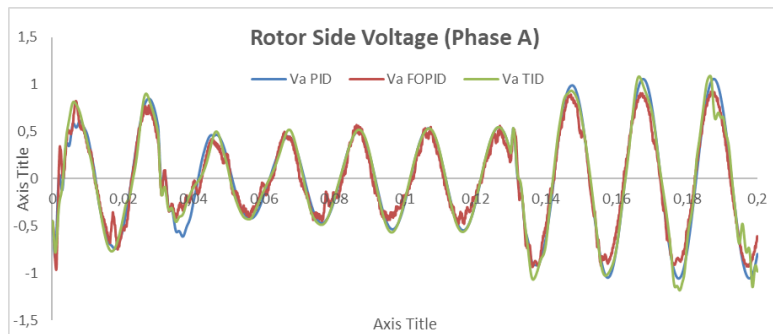


Figure 15. Rotor Side Voltage for Phase A

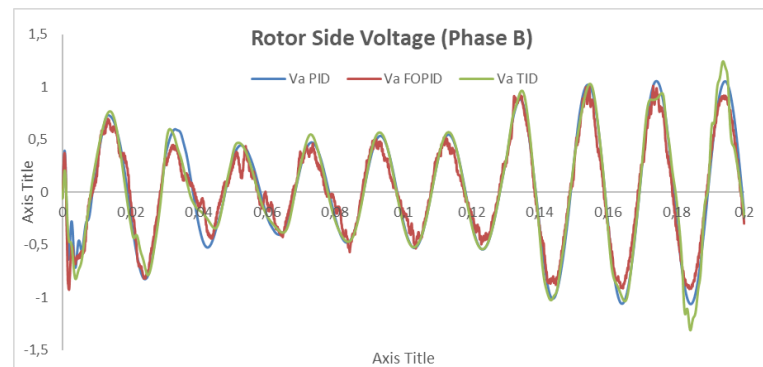


Figure 16. Rotor Side Voltage for Phase B

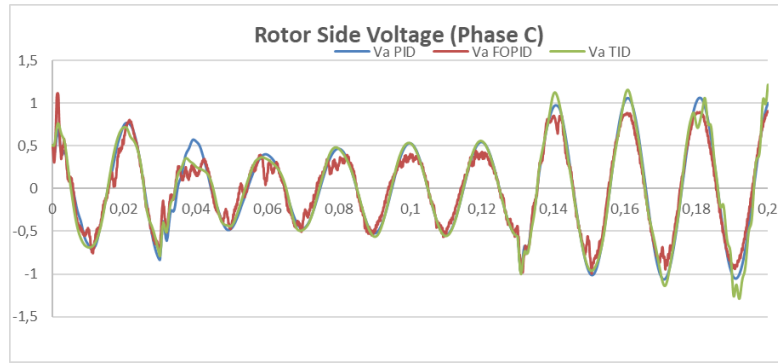


Figure 17. Rotor Side Voltage for Phase C

It can be seen from fig. 15 to fig. 17 for the rotor side voltages that the responses are the same for all controllers, but it contains more harmonics as compared to stator voltages. Among all the controllers the TID has the lowest harmonics.

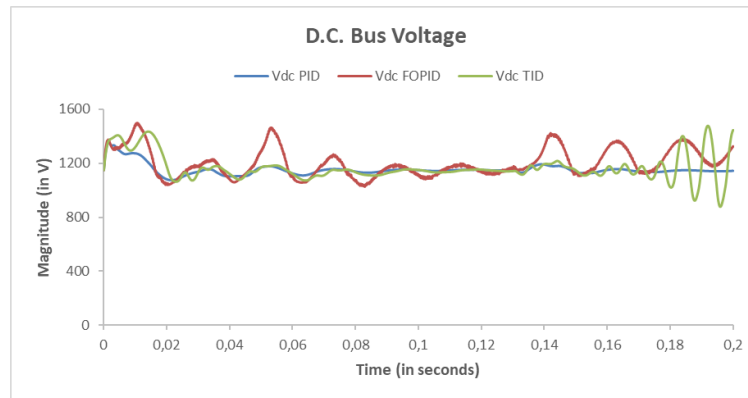


Figure 18. DC Bus Voltage

Table 2. D.C. Bus Voltage Analysis of PID, FOPID and TID Controllers

Parameters	PID Controller	FOPID Controller	TID Controller
Average Voltage	1152.460743	1203.172295	1165.095987
Maximum Voltage	1358.578166	1499.267672	1477.883833
Minimum Voltage	1075.62398	1026.485408	878.2826758

It can be observed from Table 2 that the FOPID controller gives the highest value of average voltage and the TID controller also gives better performance than PID controller. As can be seen from dc bus voltage output in fig 18 that TID controller gives a more constant output voltage as compared to FOPID. Hence it is a better controller..

The fig.19 shows the step response for the PI and PID controllers

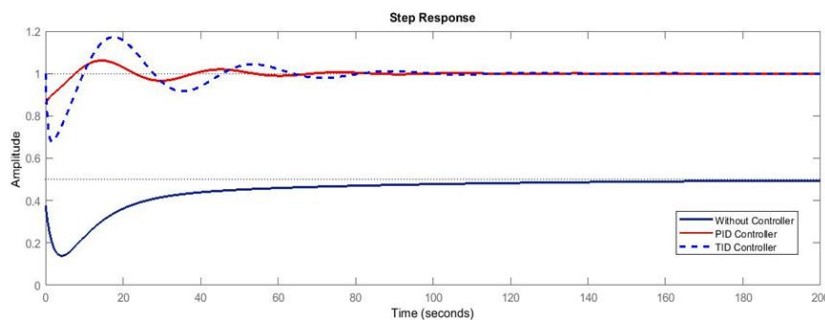


Figure 19. Step response for PI and PID Controllers

As can be observed from the step responses in the fig.19 the PI and PID converters although introduce some oscillations but the system output is close to the desired value. In case of system without any control although it is underdamped having no overshoot, but the final steady state of the system is not desired having significant error. In [5] a PID controller based on soft computational optimization techniques was analysed which although gave good performance in terms of rise time, settling time, undershoot but the output error was significantly higher

#### 4. CONCLUSION

The PI controller was optimized using Bat optimization. It reduced the settling time by more than 90% in comparison to the open loop system. It significantly reduces the settling time but the large rise time as compared to both PID and FOPID controllers' offsets it. In addition, The PID controller tuned by ALO improved the system response by reducing the rise time by 71%, the settling time by 77%, settling time by 11%, settling maximum by 8%, peak time by 97% corresponding to the step response of the open loop system. However, there is an overshoot. The FOPID controller in comparison to PID controller not only reduced the settling time further but also the settling minimum to zero. In addition, it also reduced the rise time and peak time. The FOPID controller in comparison to PI controller significantly reduces both the overshoot as well rise time. The TID controller optimized using BRO gives the best performance with respect to rise time, settling time, settling minimum, and peak time. Thus, the TID controller proposed with BRO is the best alternative for controllers' design in DFIG.

#### REFERENCES

- [1] A. Aarib, A. el Moudden, A. el Moudden, and A. Hmidat, "Control and investigation of operational characteristics of variable speed wind turbines with doubly fed induction generators," *Walailak Journal of Science and Technology*, vol. 18, no. 4, pp. 1–13, 2021, doi: 10.48048/wjst.2021.10995.
- [2] R. Thakur and R. Thakur, "Fractional Order PID Controller Design for DFIG Based Wind Energy Conversion System," in *Communications in Computer and Information Science*, 2019, vol. 956, pp. 96–105. doi: 10.1007/978-981-13-3143-5\_9.
- [3] S. Mohamed and S. Gagan, "Comparative Analysis of Controller Techniques Used in Doubly Fed Induction Generators in Wind Turbines," 2018. [Online]. Available: www.IJARIT.com
- [4] H. S. Ko, G. G. Yoon, N. H. Kyung, and W. P. Hong, "Modeling and control of DFIG-based variable-speed wind-turbine," *Electric Power Systems Research*, vol. 78, no. 11, pp. 1841–1849, Nov. 2008, doi: 10.1016/j.epr.2008.02.018.
- [5] Bharti Om, Saket R.K., and Nagar S.K., "Controller design of DFIG based wind turbine by using evolutionary soft computation technique 2017," *Engineering, Technology & Applied Science Research*, vol. 7, no. 3, pp. 1732–1736, 2017, Accessed: Jan. 11, 2022. [Online]. Available: www.etasr.com
- [6] M. Elazzaoui, "Modeling and Control of a Wind System Based Doubly Fed Induction Generator: Optimization of the Power Produced," *Journal of Electrical & Electronic Systems*, vol. 04, no. 01, 2015, doi: 10.4172/2332-0796.1000141.
- [7] Bhowmik S. and Spee R., "Wind speed estimation based variable speed wind power generation," in *Proc. 24th Annual Conf. of the IEEE*, 1998, pp. 596–601.
- [8] M. G. Simoes, B. K. Bose, and R. J. Spiegel, "Fuzzy Logic Based Intelligent Control of a Variable Speed Cage Machine Wind Generation System," 1997.
- [9] Q. Wang and L. Chang, "An intelligent maximum power extraction algorithm for inverter-based variable speed wind turbine systems," *IEEE Transactions on Power Electronics*, vol. 19, no. 5, pp. 1242–1249, Sep. 2004, doi: 10.1109/TPEL.2004.833459.
- [10] A. Miller, E. Muljadi, and D. S. Zinger, "A Variable Speed Wind Turbine Power Control," 1997.
- [11] F. Wu *et al.*, "Transfer function based equivalent modeling method for wind farm," *Journal of Modern Power Systems and Clean Energy*, vol. 7, no. 3, pp. 549–557, May 2019, doi: 10.1007/s40565-018-0410-8.
- [12] Colo.) IEEE Power & Energy Society. General Meeting (2015: Denver and Institute of Electrical and Electronics Engineers., *Power & Energy Society General Meeting, 2015 IEEE: date 26-30 July 2015*. 2015.
- [13] Z. H. Liu, H. L. Wei, Q. C. Zhong, K. Liu, X. S. Xiao, and L. H. Wu, "Parameter estimation for VSI-Fed PMSM based on a dynamic PSO with learning strategies," *IEEE Transactions on Power Electronics*, vol. 32, no. 4, pp. 3154–3165, Apr. 2017, doi: 10.1109/TPEL.2016.2572186.
- [14] S. A. Ol. da Silva, L. P. Sampaio, F. M. de Oliveira, and F. R. Durand, "Feed-forward DC-bus control loop applied to a single-phase grid-connected PV system operating with PSO-based MPPT technique and active power-line conditioning," *IET Renewable Power Generation*, vol. 11, no. 1, pp. 183–193, 2017, doi: 10.1049/iet-rpg.2016.0120.
- [15] Zooba F.A. and Bansal R., *Handbook of Renewable Energy Technology*. World Scientific.
- [16] R. Teodorescu and F. Blaabjerg, "Flexible control of small wind turbines with grid failure detection operating in stand-alone and grid-connected mode," *IEEE Transactions on Power Electronics*, vol. 19, no. 5, pp. 1323–1332, Sep. 2004, doi: 10.1109/TPEL.2004.833452.
- [17] S. M. Barakati, M. Kazerani, and J. D. Aplevich, "An overall dynamic model for a matrix converter," in *IEEE International Symposium on Industrial Electronics*, 2008, pp. 13–18. doi: 10.1109/ISIE.2008.4677115.

- [18] Krause P.C., Wasynczuk O., and Sudhoff S.D., *Analysis of Electrical Machinery*. IEEE Press, 1994.
- [19] M. Tazil *et al.*, “Three-phase doubly fed induction generators: An overview,” *IET Electric Power Applications*, vol. 4, no. 2, pp. 75–89, 2010, doi: 10.1049/iet-epa.2009.0071.
- [20] Eriksson O., *Error Control in Wireless Sensor Networks, A Process Control Perspective*. 2011.
- [21] H. Wu, M. Claypool, and R. Kinicki, “A Model for MPEG with Forward Error Correction and TCP-Friendly Bandwidth.”
- [22] Polinder H, Ferreira J.A., Jensen B.B., Abrahamsen, Atallah K, and Mc Mohan R.A., “Trends in Wind Turbine Generator Systems,” *IJEST in Power Electronics*, vol. 1, no. 3, pp. 174–185, 2013.
- [23] Bhutto D., Anasri J.A., Chachar F., Katyara S., and Soomro J., “Selection of Optimal Controller for Active and Reactive Power Control of Doubly Fed Induction Generator (DFIG),” in *2018 International Conference on Computing, Mathematics and Engineering Technologies (iCoMET)*, 2018, pp. 1–5.
- [24] T. Rahkar Farshi, “Battle royale optimization algorithm,” *Neural Computing and Applications*, vol. 33, no. 4, pp. 1139–1157, Feb. 2021, doi: 10.1007/s00521-020-05004-4.
- [25] Lazar A, Sarker R, and Abbass H, *Heuristic, and optimization for knowledge discovery*. IGI Global, 2002.
- [26] R. A. Formato, “CENTRAL FORCE OPTIMIZATION: A NEW METAHEURISTIC WITH APPLICATIONS IN APPLIED ELECTROMAGNETICS,” 2007.
- [27] E. Rashedi, H. Nezamabadi-pour, and S. Saryazdi, “GSA: A Gravitational Search Algorithm,” *Information Sciences*, vol. 179, no. 13, pp. 2232–2248, Jun. 2009, doi: 10.1016/j.ins.2009.03.004.
- [28] A. Kaveh and T. Bakhshpoori, “Water Evaporation Optimization: A novel physically inspired optimization algorithm,” *Computers and Structures*, vol. 167, pp. 69–85, Apr. 2016, doi: 10.1016/j.compstruc.2016.01.008.
- [29] A. S. Assiri, A. G. Hussien, and M. Amin, “Ant lion optimization: Variants, hybrids, and applications,” *IEEE Access*, vol. 8, pp. 77746–77764, 2020, doi: 10.1109/ACCESS.2020.2990338.
- [30] R. Eberhart and J. Kennedy, “A New Optimizer Using Particle Swarm Theory.”
- [31] A. G. Hussien, A. E. Hassanien, E. H. Houssein, M. Amin, and A. T. Azar, “New binary whale optimization algorithm for discrete optimization problems,” *Engineering Optimization*, vol. 52, no. 6, pp. 945–959, Jun. 2020, doi: 10.1080/0305215X.2019.1624740.
- [32] S. Mirjalili, “The ant lion optimizer,” *Advances in Engineering Software*, vol. 83, pp. 80–98, 2015, doi: 10.1016/j.advengsoft.2015.01.010.
- [33] X.-S. Yang, “A New Metaheuristic Bat-Inspired Algorithm,” Apr. 2010, [Online]. Available: <http://arxiv.org/abs/1004.4170>
- [34] M. Dorigo, M. Birattari, and T. Stützle, “Ant Colony Optimization.”
- [35] A. Kaveh, M. Khanzadi, M. R. Moghaddam, and M. Reza zadeh, “Charged system search and magnetic charged system search algorithms for construction site layout planning optimization,” *Periodica Polytechnica Civil Engineering*, vol. 62, no. 4, pp. 841–850, 2018, doi: 10.3311/PPci.11963.
- [36] S. Mirjalili, S. M. Mirjalili, and A. Lewis, “Grey Wolf Optimizer,” *Advances in Engineering Software*, vol. 69, pp. 46–61, 2014, doi: 10.1016/j.advengsoft.2013.12.007.
- [37] Z. W. Geem, J. H. Kim, and G. v. Loganathan, “A New Heuristic Optimization Algorithm: Harmony Search,” *Simulation*, vol. 76, no. 2, pp. 60–68, 2001, doi: 10.1177/003754970107600201.
- [38] A. H. Kashan, “League Championship Algorithm: A new algorithm for numerical function optimization,” in *SoCPaR 2009 - Soft Computing and Pattern Recognition*, 2009, pp. 43–48. doi: 10.1109/SoCPaR.2009.21.
- [39] S. Mirjalili, “Dragonfly algorithm: a new meta-heuristic optimization technique for solving single-objective, discrete, and multi-objective problems,” *Neural Computing and Applications*, vol. 27, no. 4, pp. 1053–1073, May 2016, doi: 10.1007/s00521-015-1920-1.
- [40] Goodenough J, McGuire B, and Jakob E, *Persepectives on Animal Behaviour*. John Wiley & Sons, 2009.
- [41] R. Pradhan, S. K. Majhi, J. K. Pradhan, and B. B. Pati, “Antlion optimizer tuned PID controller based on Bode ideal transfer function for automobile cruise control system,” *Journal of Industrial Information Integration*, vol. 9, pp. 45–52, Mar. 2018, doi: 10.1016/j.jii.2018.01.002.
- [42] Troy L. Best and J. D. Altringham, “BATS: BIOLOGY AND BEHAVIOUR,” *Journal of Mammalogy*, vol. 78, no. 3, pp. 986–987, 1997.
- [43] R. Thakur and R. Thakur, “Fractional Order PID Controller Design for DFIG Based Wind Energy Conversion System,” in *Communications in Computer and Information Science*, 2019, vol. 956, pp. 96–105. doi: 10.1007/978-981-13-3143-5\_9.
- [44] R. Singhal, S. Padhee, and G. Kaur, “Design of Fractional Order PID Controller for Speed Control of DC Motor,” *International Journal of Scientific and Research Publications*, vol. 2, no. 6, 2012.
- [45] J. I. Suárez, B. M. Vinagre, A. J. Calderón, C. A. Monje, and Y. Q. Chen, “LNCS 2809 - Using Fractional Calculus for Lateral and Longitudinal Control of Autonomous Vehicles,” 2003.
- [46] R. El-Khazali, “Fractional-order PI $\lambda$  D $\mu$  controller design,” *Computers and Mathematics with Applications*, vol. 66, no. 5, pp. 639–646, Sep. 2013, doi: 10.1016/j.camwa.2013.02.015.
- [47] Podlubny I., Dorcak L, and Kostial I., “On fractional derivatives, fractional-order dynamic systems and PI $\lambda$ D $\mu$  controllers.”
- [48] I. Podlubny, *Fractional Differential Equations*. 1999.
- [49] Podlubny I., “Fractional-Order Systems and -Controllers,” *IEEE Trans. Automat. Control*, vol. 44, no. 1, pp. 208–214, 1999.
- [50] D. Valério and J. Sá Da Costa, “NINTEGER: A NON-INTEGGER CONTROL TOOLBOX FOR MATLAB.”
- [51] #deepyaman Maiti, S. Biswas, and A. Konar, “Design of a Fractional Order PID Controller Using Particle Swarm Optimization Technique.”

- [52] F. Padula and A. Visioli, "Optimal tuning rules for proportional-integral-derivative and fractional-order proportional-integral-derivative controllers for integral and unstable processes," *IET Control Theory and Applications*, vol. 6, no. 6, pp. 776–786, Apr. 2012, doi: 10.1049/iet-cta.2011.0419.
- [53] A. Esgandanian and S. Daneshvar, "A Comparative Study on a Tilt-Integral-Derivative Controller with Proportional-Integral-Derivative Controller for a Pacemaker," *International Journal of Advanced Biotechnology and Research (IJBR)*, vol. 7, pp. 645–650, 2016, [Online]. Available: <http://www.bipublication.com>
- [54] W. V. Shi and M. Zhou, "Body sensors applied in pacemakers: A survey," *IEEE Sensors Journal*, vol. 12, no. 6, pp. 1817–1827, 2012, doi: 10.1109/JSEN.2011.2177256.
- [55] Lurie J. Boris and Crescenta La, "Three Parameter Tunable Tilt-Integra-Derivative (TID) Controller," 5371670, Dec. 06, 1994

## BIOGRAPHY OF AUTHORS



Mohamed Samir received the B.Tech. in Electrical Engineering, the M.Tech. in Power System from the Z.H. College of Engineering and Technology, Aligarh Muslim University, India. He is currently an Assistant Professor of Electrical Engineering with School of Engg & Technology, DIT University. His area of research interests is power system, non-renewable energy resources, distributed generation, and high voltage



**Dr. Gagan Singh** received his Graduation Degree in Electrical Engineering, M. Tech (Engineering Systems) from Dayalbagh Educational Institute, Agra, India, and PhD in Electrical Engineering from Uttarakhand Technical University in 2011. He is currently Professor of Electrical Engineering with School of Engineering & Technology, DIT University, India. He has authored a book on "Electrical Measurement & Measuring Instruments" in 2004 and has published more than thirty-two papers in conference proceedings and international journals. He has an overall experience of above twenty years. His research interests include hydropower plant instrumentation, control, modeling, and simulation.



**Dr. Nafees Ahamad** has done B.E from Madan Mohan Malaviya Engineering College, Gorakhpur, U.P., India, and a PG Diploma in computer applications from CDAC Bangalore. His master's degree (M. Tech) is in Digital Communication and his Ph.D. degree from the Department of Electrical Engineering, DIT University, India. He has vast experience of 20+ years of teaching and research and published several papers in national/international conferences and peer-reviewed journals. Recently, he is selected as a member of the preliminary design review committee for Optical Periscope & Optronic Mast for Project ICS for Submarines by Instruments Research & Development Establishment (IRDE)-A laboratory of the Defense Research & Development Organization (DRDO), Government of India. Presently, he is working with the Department of Electrical, Electronics & Communication Engineering in the capacity of Assistant Professor and Associate Head. His area of interest includes Control System, Order Reduction, Controller Design, System Engineering, Control and Automation, Electrical Machine Design, and Optimization etc.